

Dynamic Neural Networks for Jet Engine Degradation Prediction and Prognosis

S. Kiakojoori and K. Khorasani

Department of Electrical and Computer Engineering
Concordia University, Quebec, Canada

kash@ece.concordia.ca

Abstract—In this paper, fault prognosis of aircraft jet engines are considered using computationally intelligent-based methodologies to ensure flight safety and performance. Two different dynamic neural networks namely, the nonlinear autoregressive neural networks with exogenous input (NARX) and the Elman neural networks are developed and designed for this purpose. The proposed dynamic neural networks are designed to capture the dynamics of two main degradations in the jet engine, namely the compressor fouling and the turbine erosion. The health status and condition of the engine is then predicted subject to occurrence of these deteriorations. In both proposed approaches, two scenarios are considered. For each scenario, several neural networks are trained and their performance in predicting multi-flights ahead turbine output temperature are evaluated. Finally, the most suitable neural network for prediction is selected by using the normalized Bayesian information criterion model selection. Simulation results presented demonstrate and illustrate the effective performance of our proposed neural network-based prediction and prognosis strategies.

I. INTRODUCTION

Safety, cost, and performance of aircraft operations are highly dependent on gas turbine engines [1]. Jet engine prognosis problems and research have been a matter of interest in recent years due to the increasing demand on reliable operation of these systems. Fault prognosis deals with the capability of predicting the future health and state of components of a system in a fixed time horizon or their time to failure [2]. Fault prognosis information can be crucial in performing important condition-based maintenance (CBM) decisions to reduce maintenance costs as a result of unnecessary replacement of components or shut downs. In the aerospace industry, jet engines related costs constitute a large portion of the operating costs of an aircraft. Consequently, fault prognosis allows one to avoid high costs of engine failure or their overhaul.

Fault prognosis is primarily divided into two main categories, namely model-based and data driven-based approaches. Model-based approaches rely on the mathematical and physical model of the system, while data driven-based approaches are developed mostly from historical or real-time data from the system measurements for predicting the future health and state of the components. Given that generally one does not have access to an accurate mathematical model of an engine, developing model-based approaches would be a challenging task. Data driven methods use real data to represent and model the degradation of the components and predict the future behavior of the system. Moreover, inherent nonlinearities make the use of alternative computational intelligent-based

techniques as preferable and more practical. During the past few years, artificial neural networks (ANN) that rely on real and/or real-time data from the system components are mostly used as a tool for prognosis [3]. The interest in application and use of neural networks in fault prognosis is due to their ability in modelling nonlinearities of dynamical systems. The aircraft jet engine is a highly nonlinear dynamical system, therefore in order to model time delays and memory associated with the dynamics of the system, a dynamic neural network can be argued as to be required for learning its dynamics.

Various neural network methods have been used in the area of prognosis due to their flexibility in generating suitable models. Vachtsevanos and Wang [4] introduced a prognostic framework based upon the concepts of dynamic wavelet neural networks and its practicality was checked via a bearing example. Polynomial neural networks have also been used as estimation schemes for analysis of normal and defective vibration signatures in helicopter transmissions [5]. Huang *et al.* [6] predicted the life of ball bearings based on the self-organizing maps and back propagation neural network methods.

Different studies have shown the merits of ANN in terms of their faster performance as compared to conventional system identification techniques in multivariate prognosis [7] and in capturing complex phenomenon without *a priori* knowledge. Jianzhong *et al.* [8] demonstrated the concept of multiple layer perceptron (MLP) neural networks to model the remaining useful life of a NASA turbofan engine degradation simulation data set. Artificial neural networks have also been used for modeling and prediction of complex time series data [9]. In [10], Gebraeel and Lawley developed a modular neural network-based degradation model that utilizes degradation signals to determine the residual life of a degraded rolling bearing. Dragomir *et al.* [11] utilized adaptive neuro-fuzzy inference for stabilizing the error dynamics of the prognosis process. Recurrent radial basis neural networks have also been used by Zemouri for prognosis of nonlinear gas ovens [12].

Lee *et al.* [13] employed an Elman neural network for health condition prediction. Wang *et al.* [14] compared the prediction results of fault damage trend analysis using recurrent neural networks and neuro-fuzzy inference systems. They also showed the robustness of the ANN approaches in their work. Zhao *et al.* [15] developed an integrated prognostic method for gear remaining useful life prediction.

Traditionally, maintenance is performed only at the break-

downs. Thus, no analysis or planning is required, which in turn results in unscheduled downtimes [16]. Unplanned or run-to-failure maintenance is practical in industries with limited maintenance resources [17]. However, in applications such as aircraft engines, reactive maintenance causes critical problems; failure of a component may occur at an inconvenient time or it can cause damage to other parts of the system [18].

Another common maintenance technique is known as the time-based preventive maintenance, which sets a periodic interval to perform maintenance without considering the health status of the system [19]. This strategy can provide relatively higher system performance as compared to the previous approach above. However, this method is quite inefficient for and cannot handle unexpected failures. Moreover, in pre-defined maintenance policies, the system may be overhauled when it may still be in a good health condition. This leads to a resource and time consuming process that due to frequent replacements of expensive components before end of their useful life as most engineering components do not fail at periodic intervals. It is also important to determine the maintenance intervals to reduce the frequency of undesirable consequences of the system interruptions. Age-related, usage, or failure distribution have been used as means to obtain the time intervals. However, as pointed out by Luo *et al.* [20], critical system failures cannot only be determined based on the time of the system operation. Consequently, in the past ten years many utilities replace their time-based maintenance activities with efficient policies that are based on the need of the system to fulfill their needs for availability and safety [21].

In order to reduce both maintenance and repair costs and probability of the failure, condition-based maintenance (CBM) techniques have been introduced as efficient ways to increase the production cycle for modern aircraft that are based on the current health, operating and maintenance history of these systems. Variables such as vibration, temperature and acoustics can be used to collect information about the performance and behavior of the system [22].

II. NARX NEURAL NETWORK

One of the most popular model representations and structures for performing time series prediction is the nonlinear autoregressive neural network with exogenous input (NARX), where the current output value is dependent on the lagged/delayed inputs and outputs that map through the network nonlinear functions. This nonlinear transformation can be described as a feed-forward neural network, polynomial expansion, radial basis functions, wavelets, support vector machines, etc. [23].

Although recurrent architectures have feedback from hidden neurons, NARX network feedback comes only from the output neurons. Gradient-descent learning for NARX networks is more effective than in other recurrent networks due to the embedded memory of these networks that reduces the sensitivity to long-term dependencies [24]. It has also been pointed out that convergence in these networks is much faster than other networks [25]. Essentially choosing a suitable network

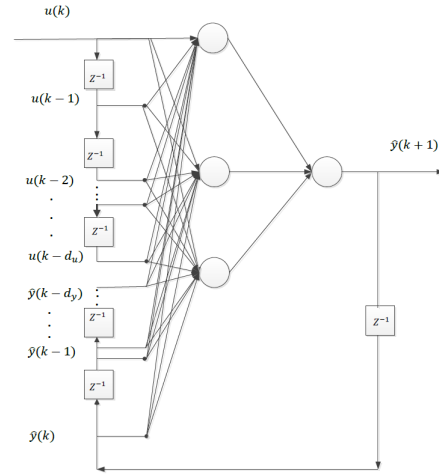


Fig. 1. NARX neural network architecture [25].

architecture in terms of the number of neurons and memory or delays are among the most important considerations for design of NARX networks that are to be used for the prediction problems.

The NARX networks use a tapped delay line from the input and delayed connections from the output layer to the input layer. In this network the estimated output (the network's output represented as $\hat{y}(k)$) is fed back to the input of the feed-forward neural network as part of the standard NARX structure as shown in Figure 1, to yield

$$\hat{y}(k+1) = f[\mathbf{y}_P(k); \mathbf{u}(k)] = f[\hat{y}(k), \dots, \hat{y}(k-d_y+1); u(k), \dots, u(k-d_u+1)], \quad (1)$$

where d_u and d_y denote the input and output delays, respectively, and f denotes the nonlinear mapping function. Equation (1) implies that the network receives the past and present values of the input as well as the past and present estimated values of the output as inputs and the next value of the output as the target in the training phase. The trained network is then used to estimate the next step value of the output for the unseen data in the testing phase.

The NARX neural network can also be trained to predict multi-steps ahead of the output based on equation (2) below where the present and the past observations $u(k), \dots, u(k-d_u+2), u(k-d_u+1)$ and the present and past estimated outputs $\hat{y}(k), \dots, \hat{y}(k-d_y+2), \hat{y}(k-d_y+1)$ are used as inputs, and the output in the n -step ahead as the target value in the training phase, that is

$$\hat{y}(k+n) = g(u(k-d_u+1), u(k-d_u+2), \dots, u(k), \hat{y}(k-d_y+1), \dots, \hat{y}(k)) \quad (2)$$

where d_u and d_y denote the input and output delays, respectively, and g denotes the nonlinear mapping function.

Dynamic back propagation algorithm is used in this paper to compute the gradients required for the network training

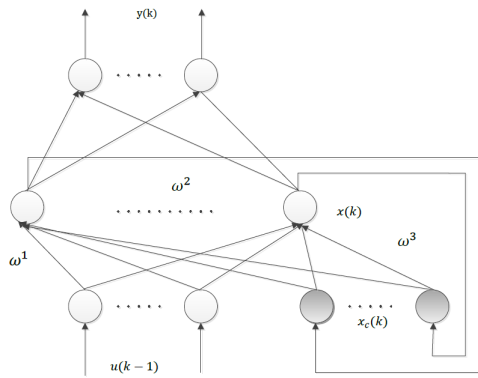


Fig. 2. Elman neural network architecture [28].

step. The weights and biases update laws use the Levenberg-Marquardt optimization scheme [26] which minimizes a combination of the squared error of the estimated and actual values of the output and weights, and then determines the optimal combination for minimizing a nonlinear performance index. These details are not included and can be found from [27].

III. ELMAN NEURAL NETWORK

An Elman neural network is in principle a regular feed-forward network with local feedback that is used to construct and introduce memory into the system. It consists of three layers, namely the input, the hidden and the output layers. In contrast to the NARX network, the output is not fed back to the input layer. Instead, special units called the context units save previous output values of the hidden layer neurons. These units are hidden in the sense that they interact exclusively with other nodes internal to the network, and not with the outside world. These values are then fed back to the input layer as additional inputs to the system [28]. An Elman network with three layers is shown in Figure 2.

At time (t), the input units receive signals in the sequence which might be a single scalar value or a vector depending on the specifics of the problem. Both the input units and the context units activate the neurons in the hidden layer. The hidden neurons then activate the output neurons. They are also fed back to activate the context units. The output is then compared with the actual one and the back propagation of the error is then used to adjust the weights. At the next time step ($t + 1$), this sequence is repeated. Therefore, the context units contain exactly the hidden neuron values at time (t). These context units thus provide the network with memory [28].

In the Elman network, the neurons of the input layer, hidden layer and output layer are fully connected by the weight matrices. Context units which save the previous values of the hidden neurons are also connected to the hidden layer through connection weights. Based on this methodology, the network output is related to the current input data as well as the past and historical input data due to the context neurons. This implies

that the output is a function of both previous activation states and current data [29].

As pointed out above, the current inputs of the hidden layer consist of input signals which are passed through the hidden layer with connection weights and the previous time steps of the hidden layer are fed back to the input layer. Following the processing of these signals in the hidden layer, they are sent to the output layer where a decision is made as to whether the output is expected or not. If the output differs from the expected one, the error is returned along with the original connection path. This iteration is repeated until the desired error for the network is achieved. These details are not included in this paper and can be found in [28].

IV. JET ENGINE MATHEMATICAL MODEL

Gas turbine engines are used in many industrial and aerospace applications. One kind of the gas turbine that is called the jet engine is a reaction engine that is used to generate high-speed thrust by the jet propulsion in accordance with Newton's laws of motion. Gas turbine performance degrades during its operation due to the deteriorations resulting from the gas path components [30]. Compressor fouling, foreign object damage (FOD), blade erosion and corrosion, worn seals, blade tip clearance increase due to wearing, etc. are among the most common causes of degradations in an engine. These degradations can then result in changes in the thermodynamic performance of the engine.

The condition or the state of components can be represented by a set of independent performance parameters. Component efficiencies and flow capacities are mostly used as performance parameters in the literature. These variables are not directly measurable, and they are thermodynamically correlated with the engine parameters such as the engine spool rotational speeds, temperatures, pressures, fuel flows, etc. [31]. Equipped with the knowledge of these observable measurements, one can determine how an engine performance differs from its healthy state.

The most popular approach for diagnostic and prognostic is known as the gas path analysis (GPA) that utilizes the above characteristics. This was introduced by Urban in 1970s [32] and was then followed up by different developments and extensions such as the optimal estimation based methods.

Based on the work of Naderi *et al.* [33] on modeling of an aircraft jet engine, a MATLAB/Simulink model for a single spool jet engine is developed. The simulation model was constructed by using mechanical, aerodynamic and thermodynamic relationships between the components of the system. Data is generated from this model under different degradation rates. These data are used to evaluate the prediction capability of the neural networks.

The information flow among different parts of a single spool jet engine is shown in Figure 3. The set of nonlinear equations corresponding to a single spool jet engine is also obtained in

V. DEGRADATION MODELING

The operation of a gas turbine is due to interactions among various components. It is affected by the wear and tear over time that can adversely impact its operation [35]. Each type of the aero-engine deterioration has an adverse effect on the performance of the aircraft, resulting in reduced thrust and increased costs [1]. It should be pointed out that due to the variety of operational and design factors for various engine components, it is usually difficult to control the speed of the degradation [35].

Degradations are usually divided into two main categories, namely: recoverable, in which the degradation mechanism can be recovered, and non-recoverable, in which the degradation mechanism cannot be recovered. The recoverable losses can be reversed by operational processes such as keeping the inlet and outlet pressures low, or the losses due to fouling that can be regained by the compressor washing. Non-recoverable degradations are the result of mechanical problems which in turn cause damage to the aerofoils. Corrosion, erosion, loss of surface finish on blades, and increased tip clearance are examples of these deteriorations [36]. After the non-recoverable losses occur, the component has to be replaced. The two most common degradations in gas turbines that are considered in this work are now described in more detail below.

A. Compressor Fouling

Compressors consume up to 60% of the power produced by turbines, therefore maintaining a compressor at its optimum performance during the operation is of significant importance. Compressor fouling is one of the main causes of the degradation of the jet engine that accounts for 70 – 85% of the total engine performance loss during its operation [37]. This degradation can primarily reduce the mass flow capacity and compressor's delivery pressure, which is then followed by the power reduction and an increase in the heat rate [38]. The reference [39] has demonstrated that fouling can reduce the mass flow rate by 5% and the output power by 13%, and an increase in the heat rate by 5.5%. This fact shows the importance of predicting the effects of the compressor fouling on the performance of the engine. Fouling is caused by the adherence of particles, such as impurities in the air, engine oil leakages or fuel impurities to the compressor blades and consequently, it increases the surface roughness, reduces the flow passage and in some cases changes the shape of the aerofoil [40].

B. Turbine Erosion

Erosion is the loss of material from the flow path by hard particles, typically larger than $10\mu m$. This is one of the main causes of the deterioration in the turbine section of the aero-engine applications. Given that the aircraft engines are typically exposed to ingestion of sand or runway materials, erosion is an important concern. Erosion decreases the turbine efficiency and increases the mass flow rate. Erosion is more important in the aero engine applications, since the particles

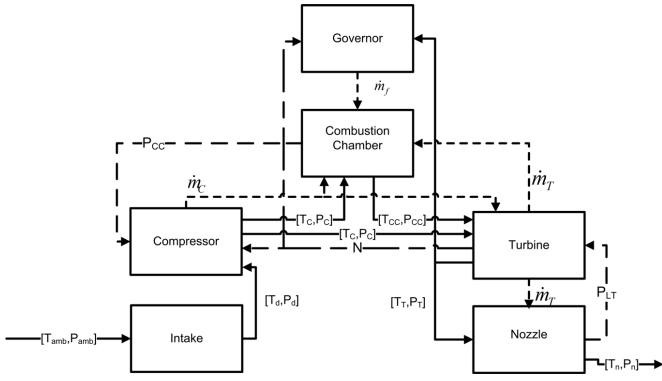


Fig. 3. Information flow diagram in a modular modeling of the jet engine dynamics.

[33] as follows:

$$\dot{T}_{CC} = \frac{1}{c_v m_{CC}} [(c_p T_C \dot{m}_C + \eta_{CC} H_u \dot{m}_f - c_p T_{CC} \dot{m}_T) - c_v T_{CC} (\dot{m}_C + \dot{m}_f - \dot{m}_T)], \quad (3)$$

$$\dot{N} = \frac{\eta_{mech} \dot{m}_T c_p (T_{CC} - T_T) - \dot{m}_C c_p (T_C - T_d)}{JN \left(\frac{\pi}{30}\right)^2}, \quad (4)$$

$$\dot{P}_T = \frac{RT_{Mi}}{V_{Mi}} (\dot{m}_T + \frac{\beta}{1+\beta} \dot{m}_C - \dot{m}_n), \quad (5)$$

$$\dot{P}_{CC} = \frac{P_{CC}}{T_{CC}} \dot{T}_{CC} + \frac{\gamma RT_{CC}}{V_{CC}} (\dot{m}_C + \dot{m}_f - \dot{m}_T), \quad (6)$$

where T_{CC} denotes the temperature in the combustion chamber, N denotes the rotor speed, m_{CC} denotes the mass flow in the combustion chamber, c_v denotes the specific heat at constant volume, c_p denotes the specific heat at constant pressure, T_C denotes the compressor temperature, \dot{m}_C denotes the compressor mass flow rate, η_{CC} denotes the combustion chamber efficiency, H_u denotes the fuel specific heat, \dot{m}_f denotes the fuel flow mass flow rate, η_{mech} denotes the mechanical efficiency, T_d denotes the diffuser temperature, \dot{m}_n denotes the mass flow rate in the nozzle, β denotes the bypass ratio, T_{Mi} denotes the mixer temperature, V_{Mi} denotes the volume of the mixer, and P_{CC} denotes the combustion chamber pressure.

The input to a single spool engine is considered as the power level angle (PLA), which is related to the mass flow rate through a variable gain. The dynamics of the fuel mass flow rate is governed by

$$\tau \frac{d\dot{m}_f}{dt} + \dot{m}_f = G u_{fd}, \quad (7)$$

where τ denotes the time constant, G denotes the gain associated with the fuel valve, and u_{fd} denotes the fuel demand which is computed by using a feedback from the rotational speed [34]. The engine model in this work has six (6) measurements namely the compressor temperature, the compressor pressure, the combustion chamber temperature, the combustion chamber pressure, the rotor speed, the turbine pressure, and finally the turbine temperature.

larger than $10\mu m$ in diameter are generally removed in the industrial gas turbine engines by using filtration systems [35].

VI. GAS TURBINE SIMULATION PROGRAM (GSP)

The gas turbine simulation program (GSP) [41] is a component-based modeling environment which allows steady-state and transient simulation of any gas turbine configuration. It was developed by the National Aerospace Laboratory (NLR). This software has been used for various applications, such as performance analysis, control system design and diagnosis [42]. It is also used for sensitivity analysis of some variables such as ambient conditions and component degradations. Moreover, flight conditions, degradation and malfunctions of the control can also be analyzed.

The GSP is used in this work to validate the degraded data that are generated with our jet engine model as provided in Section IV. A simple turbojet engine model configuration representing an engine similar to the General Electric J85 is used for the data validation which is deteriorated with the same degree as a single spool jet engine model that was described earlier in Section IV. The details for the validation simulations are not shown in this paper due to space limitations.

VII. ENGINE DEGRADATION PREDICTION PROBLEM

Both NARX and Elman neural networks are used to predict the turbine temperature for certain number of flights ahead to decide whether or not the turbine temperature exceeds certain determined thresholds at specific flight or the next flights will be safe. Data generated from a Simulink model of a single spool jet engine in presence of compressor fouling and turbine erosion are used to train and test these two neural networks. It must be noted that the data are captured at the time when the maximum fuel is applied to the engine so that the maximum thrust is provided in the aircraft *take-off mode*. In order to verify the effectiveness of these neural networks in terms of the prediction horizon, two scenarios are considered and applied to each of the models. Specifically, the compressor fouling of 3% and the turbine erosion of 3% are considered in this work. In both case studies the engine goes through the specified degradation rates in 200 simultaneous flights. Optimal neural networks are obtained by using different number of training data sets to predict 2 and 8 flights ahead turbine temperature in presence of the compressor fouling and the 5 flights ahead turbine temperature in presence of the turbine erosion.

VIII. PREDICTION RESULTS USING THE NARX NEURAL NETWORK

After an extensive set of trial and error simulation studies (not shown due to space limitations), the NARX neural networks with 3 input delays, 3 output delays, and 8 hidden neurons was found to yield the optimal performance to predict the 2 flights ahead turbine temperature. The hidden layer activation function for the NARX neural network is selected as a sigmoidal function. The selected NARX network was trained by using 80% of the available data. This implies that 160 data

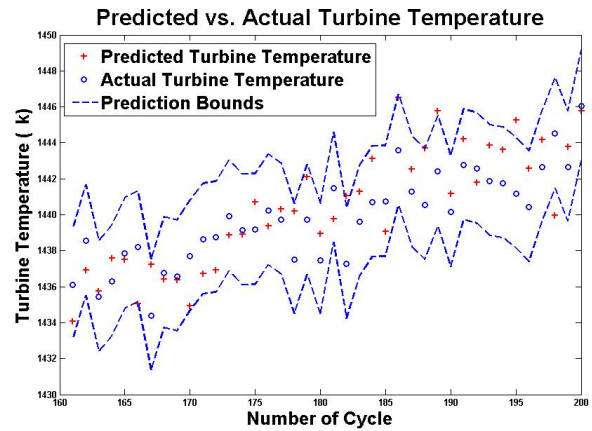


Fig. 4. The 2 step ahead predicted/actual turbine temperature along with prediction intervals using the NARX neural network in presence of the compressor fouling.

TABLE I
A 2 FLIGHT AHEAD TURBINE TEMPERATURE PREDICTION ERROR FOR COMPRESSOR FOULING USING THE NARX NEURAL NETWORK.

RMSE (K)	Standard deviation (K)	Mean (K)
2.1079	2.0649	0.5347

points (flights) are used in the training step and the remaining 40 points are used in the testing phase.

Dealing with uncertainties is inevitable. In order to overcome the problem of uncertainty in measurements, two lower and upper prediction bounds are defined to evaluate the prediction performance of the NARX network. Monte Carlo simulations are performed and according to the normal theory a multiple of the standard deviations of the prediction error (for a given confidence level that is 95%) is added and subtracted from the prediction values. When the upper bound has been reached one may declare that the engine should be taken off-line as it requires maintenance action. Predicted and actual values along with the prediction bounds are shown in Figure 4. The dashed lines show the upper and the lower prediction bounds, the cross points represent the predicted temperature while the circle points indicate the actual values. The Root Mean Squared Error (RMSE), standard deviation, and the mean of the prediction errors are summarized in Table I.

In order to predict 8 flights ahead turbine temperature in presence of the compressor fouling, we have found after an extensive set of trial and error simulation studies (not shown due to space limitations) that the NARX neural network with 7 hidden neurons has the best performance as shown in Figure 5 where the RMSE, the standard deviation, and the mean of the prediction errors are given as 3.4319 K, 3.4756 K, and 0.0146 K, respectively (these represent prediction errors that are less than 0.2% of the actual values).

To predict the turbine temperature in presence of erosion, the input and output delays are set to 3 after an extensive set of trial and error simulation studies and training (not shown due to space limitations). The NARX neural network with 7

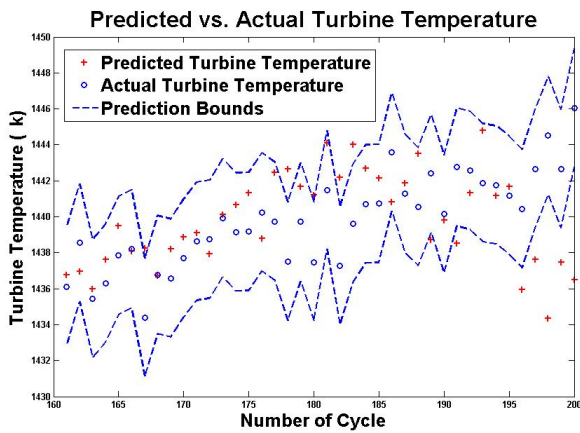


Fig. 5. The 8 step ahead predicted/actual turbine temperature along with prediction intervals using the NARX neural network in presence of the compressor fouling.

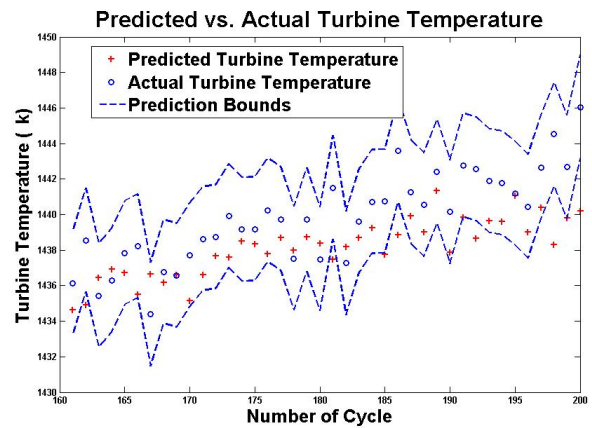


Fig. 7. The 2 step ahead predicted/actual turbine temperature along with prediction intervals using the Elman neural network in presence of the compressor fouling.

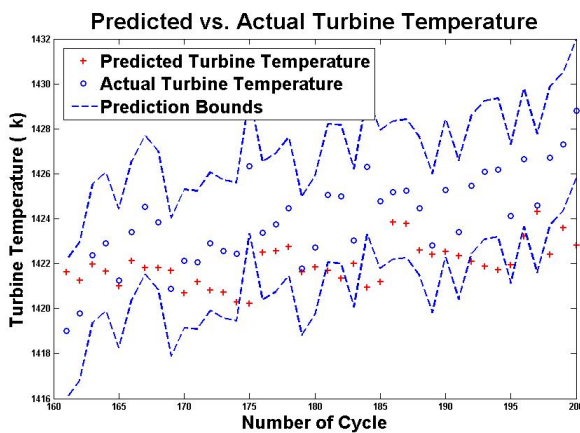


Fig. 6. The 5 step ahead predicted/actual turbine temperature along with prediction intervals using the NARX neural network in presence of the turbine erosion.

TABLE II

A 5 FLIGHT AHEAD TURBINE TEMPERATURE PREDICTION ERROR FOR TURBINE EROSION USING NARX NEURAL NETWORK.

RMSE (K)	Standard deviation (K)	Mean (K)
2.7411	1.8936	2.0044

hidden neurons was used to predict the 5 flights ahead turbine temperature. The prediction results are shown in Figure 6 along with the prediction bounds. The statistical measures of the error are tabulated in Table II.

IX. PREDICTION RESULTS USING THE ELMAN NEURAL NETWORK

The delay associated with the Elman neural network is set to 2 and the networks are trained and evaluated with the available data. It was found through extensive set of simulation studies (not shown due to space limitations) that the network with 3 hidden neurons has the best performance in the 2 flights ahead turbine temperature prediction in presence of the compressor

TABLE III
A 2 FLIGHT AHEAD TURBINE TEMPERATURE PREDICTION ERROR FOR TURBINE EROSION USING THE ELMAN NEURAL NETWORK.

RMSE (K)	Standard deviation (K)	Mean (K)
2.8646	1.7592	2.2778

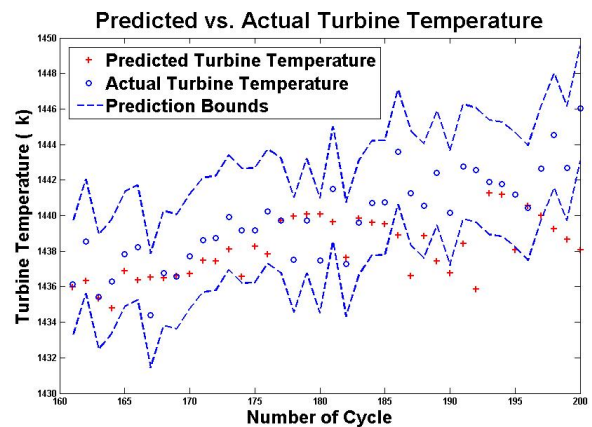


Fig. 8. The 8 step ahead predicted/actual turbine temperature along with prediction intervals using Elman neural network in presence of the compressor fouling.

fouling. This Elman network was trained using 80% of the available data points (flights). The results of the temperature prediction for the 2 flights ahead are depicted in Figure 7. The RMSE, standard deviation and mean of prediction error are summarized in Table III.

The applicability of this network in jet engine degradation prediction is also evaluated for 8 flights ahead where the predicted turbine temperatures, actual values, and prediction bounds are shown in Figure 8. The RMSE, standard deviation, and mean of the prediction error are 4.1986 K, 2.0463 K, and 2.9293 K (these represent prediction errors that are less than 0.2% of the actual value). Finally, to predict the turbine temperature in presence of erosion, the network delay is set to

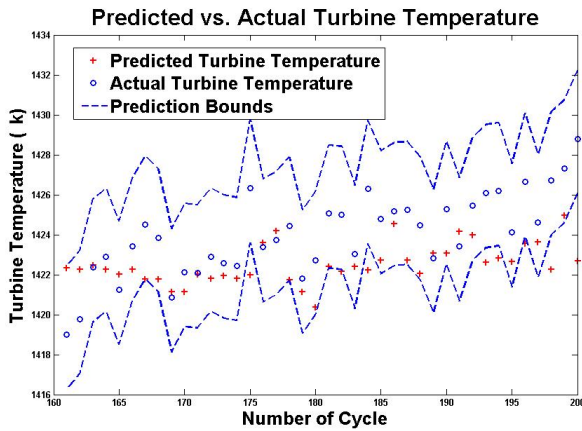


Fig. 9. The 5 step ahead predicted/actual turbine temperature along with prediction intervals using the Elman neural network in presence of the turbine erosion.

TABLE IV

A 5 FLIGHT AHEAD TURBINE TEMPERATURE PREDICTION ERROR FOR TURBINE EROSION USING THE ELMAN NEURAL NETWORK.

RMSE (K)	Standard deviation (K)	Mean (K)
2.3569	1.8783	1.4544

2 after extensive set of simulation studies (not shown due to space limitations). The network with 5 hidden neurons has the optimal prediction performance. The 5 flights ahead prediction results are shown in Figure 9 along with the prediction bounds. A summary of the statistical prediction errors are shown in Table IV.

X. COMPARISON BETWEEN THE NARX NEURAL NETWORK AND THE ELMAN NEURAL NETWORK

There should be a measure or a metric to quantitatively compare the capability of the NARX and the Elman neural networks in prediction accuracy and performance. Using an appropriate neural network can increase the accuracy of the prediction for maintenance actions but it maybe achieved at the expense of higher costs. Model selection refers to the problem of using data to select a model from a list of models [43].

Model selection should be based on the fact that it is impossible to find the “true” model that generates the data one observed. However, it should be based on a well-justified criterion to find the “best” model [44]. Model selection is a trade-off between the bias (the distance between the average prediction and the actual value) and the variance (spread of the prediction around the actual points). In other words, there is usually an improvement in the fit by increasing the parameters in the model, but at the same time parameter estimates are worse because there is less data per parameter, and there is an increase in the computational time and cost [45]. There are various model selection criteria that have been reported in the literature, namely Akaike information criterion, Bayesian information criterion, deviance information criterion, etc. [46].

Evaluation of our two proposed networks are now conducted by using the Normalized Bayesian Information Criterion

TABLE V
NBIC VALUES FOR THE NARX NEURAL NETWORK.

Degradation type	Number of flights ahead	NBIC
Compressor fouling	2	7.9979
Compressor fouling	8	8.3015
Turbine erosion	5	7.0864

TABLE VI
NBIC VALUES FOR THE ELMAN NEURAL NETWORK.

Degradation type	Number of flights ahead	NBIC
Compressor fouling	2	3.9886
Compressor fouling	8	7.9798
Turbine erosion	5	7.8085

(NBIC), which has been widely used for model identification in time-series studies [47]. Therefore, a suitable model can be found in each scenario for the purpose of performing prediction.

The NBIC can be defined as:

$$NBIC = \ln(\sigma^2) + k \frac{\ln(n)}{n} \quad (8)$$

where σ^2 denotes the variance of the prediction error, k denotes the total number of parameters in the neural network, and n denotes the number of observations. It should be noted that smaller the value for the NBIC implies that the model can predict the values better. By comparing the calculated NBIC in Table V for the NARX neural network and Table VI for the same scenario for the Elman network, one can conclude that the Elman network has lower NBIC. This implies that for the same degradation and the same training and testing data points, the Elman network outperforms the NARX network. This is mainly due to the number of parameter k that plays an important role in the calculation of the NBIC. The Elman network has a lower number of delays and hidden neurons. Thus, it can learn the trend of the degradations more efficiently and quicker than the NARX network.

XI. CONCLUSION

In this paper, we have proposed two computationally intelligent-based approaches for fault prognosis of the aircraft jet engine. The reliability and performance of these networks are evaluated to predict the turbine temperature under the multi-flights ahead scenarios and in presence of various deteriorations and degradations in the engine such as compressor fouling and turbine erosions. The prediction capabilities of our proposed neural networks are compared. The first prediction scheme is based on the use of the nonlinear autoregressive neural network with exogenous input (NARX). The second prediction scheme is based on the use of the Elman neural networks. The capabilities of the NARX and the Elman neural networks are compared by using the normalized Bayesian information criterion. The results show that for the same degradation and the same training and testing data points the Elman neural network outperforms the NARX neural network

for performing the prediction and health prognosis of an aircraft jet engine.

REFERENCES

- [1] M. Naem, R. Singh, and D. Probert, "Implications of engine deterioration for fuel usage," *Applied Energy*, vol. 29, no. 1, pp. 125–146, 1998.
- [2] T. Brotherton, G. Jahns, J. Jacobs, and D. Wroblewski, "Prognosis of faults in gas turbine engines," 2000.
- [3] A. Heng, S. Zhang, A. C. Tan, and J. Mathew, "Rotating machinery prognostics: State of the art, challenges, and opportunities," *Rotating machinery prognostics: State of the art, challenges, and opportunities*, vol. 23, no. 3, pp. 724–739, 2009.
- [4] G. Vachtsevanos and P. Wang, "Fault prognosis using dynamic wavelet neural network," 2001.
- [5] B. E. Parker, T. M. Nigro, M. P. Carley, R. L. Barron, D. G. Ward, H. V. Poor, D. Rock, and T. A. DuBois, "Helicopter gearbox diagnostics and prognostics using vibration signature analysis," vol. 1965, pp. 531–542, 1993.
- [6] R. Huang, L. Xi, X. Li, C. R. Liu, H. Qiu, and J. Lee, "Implications of engine deterioration for fuel usage," *Applied Energy*, vol. 59, no. 2, pp. 125–146, 1998.
- [7] J. Lee, "A systematic approach for developing and deploying advanced prognostics technologies and tools: methodology and applications," Harrogate, UK, 2007.
- [8] S. Jianzhong, Z. Hongfu, Y. Haibin, and M. Pecht, "Study of ensemble learning-based fusion prognostics," Macau, 2010.
- [9] G. Xue, L. Xiao, M. Bie, and S. Lu, "Fault prediction of boilers with fuzzy mathematics and rbf neural network," *Communications, Circuits and Systems*, vol. 2, pp. 1012–1016, 2005.
- [10] N. Z. Gebrael and M. A. Lawley, "A neural network degradation model for computing and updating residual life distributions," *IEEE Transactions on Automation Science and Engineering*, vol. 5, no. 1, pp. 154–163, 2008.
- [11] O. Dragomir, R. Gouriveau, and N. Zerhouni, "Adaptive neuro-fuzzy inference system for mid term prognosis error stabilization," *International Journal of Computers, Communications & Control*, vol. 1, p. 6, 2008.
- [12] R. Zemouri, "Recurrent radial basis function network for time-series prediction," *Engineering Application of Artificial Intelligence*, vol. 16, no. 5, pp. 453–463, 2003.
- [13] J. Lee, J. Ni, D. Djurdjanovic, H. Qiu, and H. Liao, "Intelligent prognostics tools and e-maintenance," *Computers in industry*, vol. 54, no. 1, pp. 476–489, 2006.
- [14] W. Q. Wang, M. F. Golnaraghi, and F. Ismail, "Prognosis of machine health condition using neuro-fuzzy systems," *Mechanical Systems and Signal Processing*, vol. 18, no. 4, pp. 813–831, 2004.
- [15] F. Zhao, Z. Tian, and Y. Zeng, "Uncertainty quantification in gear remaining useful life prediction through an integrated prognostics method," *IEEE Transactions on Reliability*, vol. 62, no. 1, pp. 146–159, 2013.
- [16] A. Jardine, D. Lin, and D. Banjevic, "A review on machinery diagnostics and prognostics implementing condition-based maintenance," *Mechanical Systems and Signal Processing*, vol. 20, no. 7, pp. 1483–1510, 2006.
- [17] L. R. Contreras, C. Modi, and A. Pennathur, "Integrating simulation modelling and equipment condition diagnostics for predictive maintenance strategies - a case study," *Proceedings of the Winier Simulation Conference*, 2002.
- [18] P. C. Escher, "Pythia: An object-oriented gas path analysis computer program for general applications," Cranfield University, Cranfield, October 1995.
- [19] H. C. Pusey, "Turbomachinery condition monitoring and failure prognosis," *SAVIAC/Hi-Test Laboratories*, Winchester, Virginia, March 2007.
- [20] J. Luo, K. Pattipati, L. Qiao, and S. Chigusa, "Model-based prognostic techniques applied to a suspension system," *IEEE Transactions on Systems, Man and Cybernetics*, vol. 38, no. 5, pp. 1156–1168, 2008.
- [21] J. Endrenyi, S. Aboresheid, and R. N. Allan, "The present status of maintenance strategies and the impact of maintenance on reliability," *IEEE Transactions on Power Systems*, vol. 16, no. 4, pp. 638–646, 2001.
- [22] S. Azirah Asmai, B. Hussin, and M. Mohd Yusof, "A framework of an intelligent maintenance prognosis tool," *Second IEEE International Conference on Computer Research and Development*, pp. 241–245, 2010.
- [23] J. Sjoberg, Q. Zhang, L. Ljung, A. Benveniste, B. Delyon, P. Glorennec, H. Hjalmarsson, and A. Juditsky, "Non-linear black-box modelling in system identification: a unified overview," *Automatica*, vol. 31, no. 12, pp. 1691–1724, 1995.
- [24] B. Horne and C. Gilles, "An experimental comparison of recurrent neural networks," *Neural Information Processing Systems*, vol. 7, pp. 697–704, 1995.
- [25] Y. Gao and M. Er, "Narmax time series model prediction: feedforward and recurrent fuzzy neural network approaches," *Fuzzy Sets and Systems*, vol. 150, no. 2, pp. 331–350, 2005.
- [26] E. Diaconescu, "The use of narx neural network to predict chaotic time series," *WSEAS Transactions on Computer Research*, vol. 3, no. 3, pp. 182–191, 2008.
- [27] C. Jiang and F. Song, "Sunspot forecasting by using chaotic time-series analysis and narx network," *Journal of Computers*, vol. 6, no. 7, pp. 1424–1429, 2011.
- [28] J. L. Elman, "Finding structure in time," *Cognitive Science*, vol. 14, no. 2, pp. 179–211, 1990.
- [29] C. Liu, D. Jiang, and M. Zhao, "Application of rbf and elman neural networks on condition prediction in cbm," *Proc. of the Sixth Int. Symposium on Neural Networks*, pp. 847–855, Springer-Verlag 2009.
- [30] Y. G. Li, "Performance analysis based gas turbine diagnostics: A review," *Journal of Power and Energy*, vol. 216, no. 5, pp. 363–377, 2002.
- [31] S. Ogaji, S. Sampath, R. Singh, and S. D. Probert, "Parameter selection for diagnosing a gas-turbines performance-deterioration," *Applied Energy*, vol. 73, no. 1, pp. 25–46, 2002.
- [32] L. A. Urban, "Parameter selection for multiple fault diagnostics of gas turbine engines," *Journal of Engineering for Power*, vol. 97, no. 2, 1974.
- [33] E. Naderi, N. Meskin, and K. Khorasani, "Nonlinear fault diagnosis of jet engines by using a multiple model based approach," *Journal of Engineering for Gas Turbines and Power*, vol. 134, no. 1, 2012.
- [34] S. M. Camporeale, B. Fortunato, and M. Mastrovito, "A modular code for real time dynamic simulation of gas turbines in simulink," *Journal of Engineering for Gas Turbines and Power*, vol. 128, no. 3, pp. 506–517, 2006.
- [35] R. Kurz and K. Brun, "Degradation in gas turbine systems," *Proceedings of the International Gas Turbine & Aeroengine Congress & Exhibition*, Munich, Germany, 2000.
- [36] S. M. Flesland, "Gas turbine optimum operation," *Master of Science in Product Design and Manufacturing*, Norwegian University of Science and Technology, December 2010.
- [37] A. Zwebek, "Combined cycle performance deterioration analysis," *PhD Thesis, Cranfield University*, 2002.
- [38] G. F. Aker and H. I. Saravanamuttoo, "Predicting gas turbine performance degradation due to compressor fouling using computer simulation techniques," *Journal of Engineering Gas Turbines Power*, vol. 111, no. 2, pp. 343–400, 1989.
- [39] C. B. Meher-Homji and A. Bromley, "Gas turbine axial compressor fouling and washing," *Proceedings of the Turbomachinery Symposium*, 2004.
- [40] Z. Mustafa, "Analysis of droplets in compressor gas turbines," *PhD Thesis, Cranfield University, UK*, 2006.
- [41] W. P. J. Visser, O. Kogenhop, and M. Oostveen, "A generic approach for gas turbine adaptive modeling," *Journal of Engineering for Gas Turbines and Power*, vol. 128, no. 1, pp. 13–19, 2006.
- [42] W. P. Visser and M. J. Broomhead, "Gsp: A generic object-oriented gas turbine simulation environment," *National Aerospace Laboratory (NLR)*, 2000.
- [43] H. Acquah, "Comparison of akaike information criterion (aic) and bayesian information criterion (bic) in selection of an asymmetric price relationship," *Development and Agricultural Economics*, vol. 2, no. 1, pp. 1–6, 2010.
- [44] K. P. Burnham and D. R. Anderson, "Multimodel inference understanding aic and bic in model selection," *Sociological Methods and Research*, vol. 33, no. 2, pp. 261–304, 2004.
- [45] D. Posada and T. R. Buckley, "Model selection and model averaging in phylogenetics: Advantages of akaike information criterion and bayesian approaches over likelihood ratio tests," *Systematic Biology*, vol. 53, no. 5, pp. 793–808, 2004.
- [46] K. Hirose, S. Kawano, S. Konishi, and M. Ichikawa, "Bayesian information criterion and selection of the number of factors in factor analysis models," *Journal of Data Science*, vol. 9, no. 2, pp. 243–259, 2011.
- [47] E. Schwarz and E. Gideon, "Estimating the dimension of a model," *Annals of Statistics*, vol. 6, no. 2, pp. 461–464, 1978.